Microscopic Tunneling Spectroscopy on High-Temperature Superconductors

Koichi Kitazawa

Tunneling spectroscopy, which was crucial in proving the existence of the Bardeen-Cooper-Schrieffer (BCS) mechanism in conventional superconductors, has been limited in its usefulness for studying high transition temperature (T_c) superconductors. This is a consequence of the difficulty of obtaining an ideal tunneling junction for these materials, which exhibit extremely short coherence lengths and nonhomogeneous electronic structures (*1*). Recent improvements in cryogenic scanning tunneling microscopy (STM), however, including operation under controlled atmosphere and preparation of a fresh surface in situ at cryogenic temperatures (*2*, *3*), may change this. This work seems to be restoring the power of local tunneling spectroscopy to discriminate among the relative contributions to superconductivity from each of the atomic positions in the superconducting crystal structure.

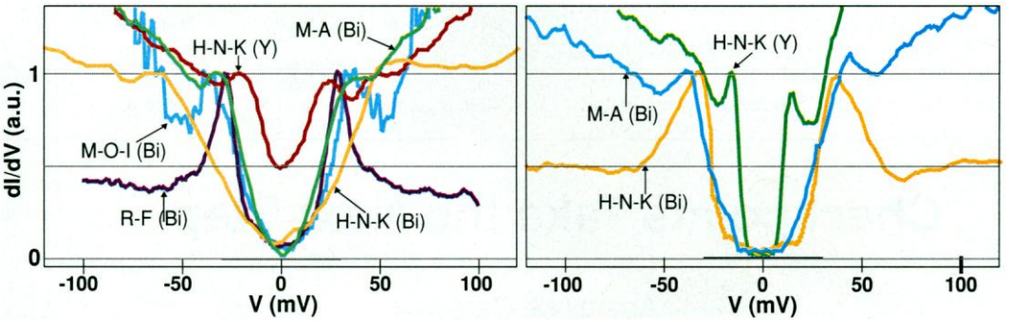

Spectral shapes. Comparison of tunneling spectra for several high-T_c superconductors (*4*–*8*). The spectra fall into two broad categories: type A (left), with curved slope in the gap region, and type B (right), which are flat and low near zero bias. All of the spectra are taken on the basal plane (001) of the layered structure and are shown in units of dI/dV (I, current; V, voltage), which correspond directly to the single-particle density of states. (Bi) and (Y) designate results taken on Bi 22/2 and YBCO, respectively. H-N-K (Bi) (4), R-F (5), M-O-I (6), M-A (7), and H-N-K (Y) (8) stand for the initials of the authors.

Until 1991, tunneling results on high-T_c materials had been irreproducible, and there had been little consensus as to which features of the superconducting gap spectrum were important. As atomic resolution was attained with STM imaging for vacuum gap conditions between the STM tip and the sample, the tunneling spectra of the high-T_c superconductors converged except for the details. Typical superconducting gap spectra observed by several groups who have achieved vacuum gap conditions (*4*–*8*) are compared in the figure.

The superconducting gap energy Δ is in the extreme strong coupling regime, with $2\Delta/k_BT_c$ = 6 to 9, compared with the BCS weak coupling value of 3.52. The gap structure cannot be fit by the BCS theory or by its modified version (*9*). In particular, the slope just inside the gap peak is much less steep than expected. The results therefore indicate the extraordinary nature of the gap structure of the high-T_c superconductors if analyzed within the framework of BCS superconductivity, which is characterized by *s*-wave symmetry for the Cooper pair wave function. The *s*-wave, isotropic in the momentum space, should raise a tunneling spectrum of a well-defined gap structure with a finite opening—that is, steep walls and essentially zero conductance inside the gap.

Several aspects of the spectra are still controversial. (i) The spectrum outside the gap is reported to be either V-shaped or flat. This is a matter of interest because a flat background is expected for a Fermi liquid, whereas a V-shaped excitation spectrum has been discussed in terms of a non-Fermi liquid. (ii) The low-lying excitation spectrum near zero bias is another point of hot argument. The "type A" spectra (left panel of the figure) are better fit by assuming the presence of a line node in the gap structure in the two-dimensional momentum space, and thus indicating either *d*- or extended *s*-wave symmetry for the pairing mechanism. On the other hand, the "type B" spectra (right panel) instead show flat and low bottoms near zero bias, indicating a finite opening of the superconducting gap and hence supporting at least a partial contribution from the *s*-wave. Therefore, one of the two types of results must be picking up the nonintrinsic signal. In the former type, the atomic arrangement is observable on the surface (CuO chain layer for YBCO and BiO layer for Bi2212), whereas in the latter type (which are observed much less frequently), the spectra are taken on the surfaces that lose the atomic contrast.

Researchers who reported the type B results also observed the spectra of type A on the surfaces where the atomic arrangement was observable. Therefore, the difference in the results must be attributable to the difference in the top surface layers. The type B spectra may be the result of surface degradation created either by surface defects or by adsorption of molecules from gaseous phase. On the other hand, those who report the type B results claim that the surface observed in the type B cases is the superconducting CuO_2 plane (or that covered by a BaO or SrO monatomic layer). Hence, the spurious current to the nonsuperconducting layers that cover the surface, such as the CuO chains or the BiO layer, can be avoided. They also speculate that the superconducting surface is difficult to image as a result of its higher homogeneous conductance (*10*).

Indeed, Murakami *et al.* (*7*) caught an STM image of three terraces of which two were BiO layers with a one step difference in height; the third one, intermediate in height and hence unlikely to be a BiO layer, did not give the atomic image. The type B spectra were obtained on the intermediate terrace, whereas type A was obtained on the two BiO layers. Therefore, the details of tunneling spectra must be sensitive to the very top structure of the surface in high-temperature superconductors.

Recent theories have predicted various possibilities about the surface nature of a *d*-wave superconductor: (i) the formation of a surface *s*-wave region attributable to surface reflection of the carriers (*11*, *12*), (ii) angular dependence of tunneling conductance (*13*), and (iii) a new symmetry and excitation spectrum of the vortex core structure (*14*). Among those making the further experimental efforts along this line, Renner and Fischer have succeeded in observing images of vortex lattice for the first time on high-temperature superconductors, demonstrating that excitation spectra can be obtained inside the vortex core (*15*).

Information to atomically pinpoint the local functions in the complex structure is

The author is in the Department of Applied Chemistry, University of Tokyo, 7-3-1 Hongo, Bunkyo-ku, Tokyo, Japan. E-mail: supercom@tansei.cc.u-tokyo.ac.jp

provided by STM spectroscopy. After comparing the STM atomic images at various bias voltages on the edge plane of the layer structure, Hasegawa *et al.* claimed that the BiO layer in Bi2212 (*16*) is insulative with gap energy several tens of millielectron volts or larger. This finding was contrary to the conclusions indicated by the band calculations and photoelectron spectroscopy. However, the insulative nature of the BiO layer has gradually been established by the observation of the S-I-S (superconductor-insulator-superconductor) type Josephson junction characteristics in the built-in layer structure (*17*) and by the most recent electron spectroscopy results (*18*). The CuO chain in YBCO was also found by the same method to exhibit a much lower density of states near the Fermi level (*19*).

Furthermore, the CuO chain, which was once believed to be the highly conductive path that gives the conductance anisotropy in the basal plane in YBCO, may form a charge density wave (CDW) with a wavelength several times the bond length of CuO (*20*). Such a wave is suggested by comparison of atomic images taken at different bias voltages, which yield the alternative appearance and disappearance of the CuO chain image along the crest and trough of a CDW on reversal of the sign of the bias voltage.

Thus, atomic site tunneling spectroscopy has emerged as a potential tool with which we can obtain excitation spectra of electrons as a function of atomic location—a new concept in solid-state physics.

References

1. T. Hasegawa, H. Ikuta, K. Kitazawa, in *Physical Properties of High Temperature Superconductors III*, D. M. Ginsberg, Ed. (World Scientific, Singapore, 1992), pp. 523–621.
2. H. L. Edwards, J. T. Markert, A. L. de Lozanne, *J. Vac. Sci. Technol.* **B12**, 1886 (1994).
3. R. R. Shulz and C. Rossel, *Rev. Sci. Instrum.* **65**, 1918 (1994).
4. T. Hasegawa, M. Nantoh, K. Kitazawa, *Jpn. J. Appl. Phys.* **30**, L276 (1991).
5. Ch. Renner and O. Fischer, *Phys. Rev.* **B51**, 9208 (1995).
6. C. Manabe, M. Oda, M. Ido, *Physica* **C235-240**, 797 (1994); *Phys. Rev.*, in press.
7. H. Murakami and R. Aoki, *J. Phys. Soc. Jpn.* **64**, 1287 (1995).
8. M. Nantoh *et al.*, *J. Appl. Phys.* **75**, 5227 (1994).
9. R. C. Dynes, V. Narayanamurti, J. P. Garno, *Phys. Rev. Lett.* **41**, 1509 (1978).
10. K. Kitazawa *et al.*, *Physica* **C209**, 23 (1993).
11. M. Matsumoto and H. Shiba, *J. Phys. Soc. Jpn.* **64**, 3384 and 4867 (1995).
12. K. Kuboki and M. Sigrist, *ibid.*, in press.
13. Y. Tanaka and S. Kashiwaya, *Phys. Rev. Lett.* **24**, 3451 (1995).
14. N. Schopohl and K. Maki, *Phys. Rev.* **B52**, 490 (1995); A. J. Berlinsky, A. L. Fetter, M. Franz, C. Kallin, P. I. Soininen, *Phys. Rev. Lett.* **75**, 2200 (1995).
15. I. Maggio-Aprile, Ch. Renner, A. Erb, E. Walker, O. Fischer, *Phys. Rev. Lett.* **75**, 2754 (1995).
16. T. Hasegawa and K. Kitazawa, *Jpn. J. Appl. Phys.* **29**, L434 (1990).
17. K. Tanabe, Y. Hidaka, S. Karimoto, M. Suzuki, *Phys. Rev.*, in press.
18. P. Aebi *et al.*, *Phys. Rev. Lett.* **72**, 2757 (1994).
19. M. Nantoh *et al.*, *Physica* **C242**, 277 (1995).

Checkpoints Take the Next Step

Antony M. Carr

Treatment of dividing cells with radiation causes a pause in the G_2 phase of the cell cycle that stops the cell from proceeding through mitosis. When the pause is absent, the cells are more sensitive to radiation (*1*). These observations led to the concept of "checkpoints"—specific times within the cell cycle during which progression through the cycle can be delayed in response to either DNA damage or to incompletion of prior cell cycle events such as DNA replication. Several checkpoints monitor the integrity of the DNA: Radiation damage to DNA can delay the start of a new cell cycle (G_1-S checkpoint), DNA damage delays DNA synthesis (S phase progression checkpoint), DNA damage delays mitosis (DNA damage checkpoint), and errors in, or delays to, DNA synthesis delay mitosis (S-M checkpoint). Many proteins of the checkpoint pathways have been identified by genetic analysis of yeast (*2*), but the corresponding biochemical changes associated with their activation have not been analyzed. Two reports in this issue have now initiated the biochemical study of mitotic checkpoint pathways in yeast (*3*, *4*).

The Chk1 protein of fission yeast, a putative kinase, is required for mitotic arrest after DNA damage, but not for mitotic arrest when DNA synthesis is inhibited (*5*).

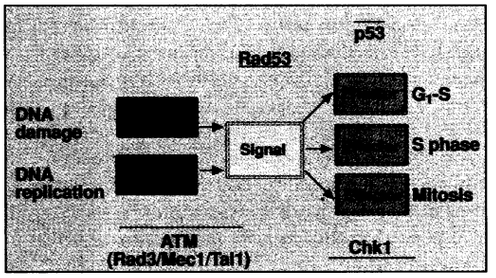

Checkpoint pathways: a detector, signal, and effector. The ATM family of proteins is probably part of the detector of DNA damage that stops cell cycle progression, whereas the Rad53 protein may be part of the signal pathways that activate the effectors such as Chk1 (mitosis) and possibly p53 (G_1-S transition).

Walworth and Bernards (*3*) have now demonstrated that Chk1 is phosphorylated in response to DNA damage but not when the S phase is inhibited by hydroxyurea, thus correlating the activation of a checkpoint pathway to a biochemical modification of a checkpoint protein. Mitotic checkpoints require three distinct functions: a detection system to determine the change in DNA structure; a signal pathway to transmit this information; and an effector mechanism to interact with the cell cycle machinery (see the figure). Genetic analysis of *chk1* mutants suggested that Chk1 functions as part of the effector mechanism, close to the cell cycle machinery (*5*, *6*). By examining the phosphorylation status of Chk1 after irradiation of various checkpoint mutants, Walworth and Bernards have formally placed Chk1 downstream of the majority of the fission yeast checkpoint proteins, consistent with such a role.

One of the checkpoint proteins upstream of Chk1 is Rad3, a large member of the phosphatidylinositol-3′ subgroup of kinases (*7*). The *rad3* protein shares significant amino acid homology with the human ATM protein, which is mutated in patients with the cancer-prone genetic disorder ataxia telangiectasia (*8*). Cells from patients with this disease show a phenotypic overlap with *rad3* mutants, suggesting functional as well as structural conservation. *Saccharomyces cerevisiae* has two gene products that are related to the ATM protein: Mec1, an essential protein required for the mitotic checkpoints and the homolog of *Schizosaccharomyces pombe* Rad3; and Tel1, which is involved in telomere maintenance. Although Tel1 mutants are not defective in checkpoints, Mec1 and Tel1 share some overlapping functions (*4*, *9*). Sanchez and co-workers (*4*) have now shown that the *RAD53* gene can act as a multicopy suppressor of *mec1*$^-$ lethality. Rad53 is required for DNA damage checkpoints and for the S phase–mitosis checkpoint, and it is also needed for the transcriptional response to DNA damage. In their re-

The author is with the Medical Research Council Cell Mutation Unit, Sussex University, BN1 9RR, UK. E-mail: a.m.carr@sussex.ac.uk